NASA CONTRACTOR REPORT

NASA CR-1449

NON-LINEAR LONGITUDINAL DYNAMICS OF AN ORBITAL LIFTING VEHICLE

by Nguyen X. Vinh and Arthur J. Dobrzelecki

Prepared by
UNIVERSITY OF MICHIGAN
Ann Arbor, Mich.
for

NATIONAL AERONAUTICS AND SPACE ADMINISTRATION • WASHINGTON, D. C. • OCTOBER 1969

NASA CR-1449

NON-LINEAR LONGITUDINAL DYNAMICS OF AN ORBITAL LIFTING VEHICLE

By Nguyen X. Vinh and Arthur J. Dobrzelecki

Prepared under Contract No. NASr 54(06) by
UNIVERSITY OF MICHIGAN
Ann Arbor, Mich.

for

NATIONAL AERONAUTICS AND SPACE ADMINISTRATION

For sale by the Clearinghouse for Federal Scientific and Technical Information
Springfield, Virginia 22151 – CFSTI price $3.00

TABLE OF CONTENTS

LIST OF FIGURES

NOTATION

$A, B, C,$	= principal moments of inertia
$a, b, c, d,$	= numerical coefficients, Eq. (64)
a	= correctional factor, Eq. (27)
C_D	= drag coefficient
C_L	= lift coefficient
C_m	= pitching moment coefficient
$C_{D_\alpha}, C_{L_\alpha}, C_{m_\alpha}, C_{m_{\hat{q}}}$	= stability derivatives
C_{N_1}	= coefficient, Eq. (48)
C_{N_2}	= coefficient, Eq. (54)
g	= acceleration due to gravity
h_1	= correctional coefficient, Eq. (41)
k_y	= radius of gyration in pitch
k_0	$= \frac{A - C}{B}$
K	= coupling coefficient, Eq. (54)
L	= mean chord, characteristic length
m	= mass of vehicle
n	= angle-of-attack frequency
q	= angular velocity in pitch relative to the earth
$\hat{q}$	$= \frac{L}{2u_0} q$
r	= radial distance from center of earth
$\hat{r}$	$= \frac{r}{r_0}$
s	$= \frac{u_0}{\sqrt{g_0 r_0}}$, speed ratio
S	= reference area
t	= time
$\hat{t}$	$= \frac{g_0}{u_0} t$
$\hat{u}$	$= \frac{V}{u_0}$
T	= thrust, period
u_0	= reference circular speed

W = vehicle weight

V = speed along the orbit

X = vector state, Eq. (13)

x = $\cos \tau$

α = angle-of-attack

β = density coefficient Eq. (11)

γ = flight path angle

δ = $\left(\frac{L}{2k_y} \right)^2$

ϵ = small perturbation, eccentricity of orbit

η = $\frac{2r_0}{L}$

θ = angle of pitch

λ = characteristic value

μ = $\frac{\rho_0 S u_0^2}{2mg_0}$

ξ = density coefficient Eq. (24)

ρ = air mass density

σ = non-dimensional density gradients Eq. (10)

τ = $\omega \hat{t} = \frac{\omega g_0}{u_0} t$

ϕ = central range angle (Fig. 1), function, Eq. (66)

ω = phugoid frequency

Subscript

$( )_0$ = reference flight path

$( )_i$ = perturbed quantity

ABSTRACT

This paper presents an analytical study of the longitudinal dynamics of a thrusting, lifting, orbital vehicle in a nearly circular orbit. The translational motion is composed of a non-linear oscillation, or phugoid, and a spiral mode which results in either decay or dilatation of the orbit depending on the perturbed initial conditions. The non-linear effects on the phugoid period and damping are small in the altitude range considered. Elements of the orbit such as radial distance, velocity, and flight path angle were obtained explicitly as functions of time. The behavior of the variations of these elements is correctly predicted. Explicit expressions for period and damping of the angle-of-attack mode were derived. It is shown that a critical altitude may exist at which the phugoid mode and the angle-of-attack mode have nearly equal periods. Near this resonance altitude linearized solutions are no longer valid and a study of the non-linear equations shows that there is a strong interaction between the translational and the rotational modes resulting in a switching of the two frequencies of oscillations.

NON-LINEAR LONGITUDINAL DYNAMICS OF AN ORBITAL LIFTING VEHICLE

INTRODUCTION

In Ref. 1, Etkin has presented a very enlightening study of the small-perturbation dynamics of a satellite vehicle in a nearly circular orbit. He linearized the equations of motion and solved the resulting fifth-order system numerically. It was found that the linear solutions contain two oscillating components which can be identified with the classical phugoid and short-period modes and a new spiral mode. Etkin then showed by direct numerical calculations that, with hypersonic speeds at a flight altitude where the gravity torque predominates over the aerodynamic torque, the so-called short-period oscillations can develop a period that is longer than that of the corresponding phugoid. At the critical resonance altitude where the two periods are nearly equal, Etkin's linearlized solutions are no longer valid because the amplitudes of the oscillations are large.

More recently, E. V. Laitone and Y. S. Chou made a theoretical analysis of the same problem.[2] Their analytical solution of the linear equations are in excellent agreement with Etkin's numerical calculations.

In this paper, we extend Laitone and Chou's investigation to include non-linear effects in the longitudinal dynamics of the orbiting vehicle. The equations of motion of a thrusting, lifting vehicle in a nearly-circular orbit are integrated directly in matrix form, using a perturbation technique. It will be shown that, for the phugoid, or trajectory mode, Etkin's new spiral mode is the familiar secular perturbation of a vehicle flying in a resisting medium. The proper phugoid motion, with damping, is described by oscillatory terms with diminishing amplitudes. Through explicit formulas, the asymptotic behaviors of the variations of the elements of the orbit are correctly predicted. Furthermore, a very simple formula yields a value for the altitude where variations in velocity change sign. This value for the velocity inversion altitude is accurate to within 10 feet of the numerically computed value. For the short-period mode, which we shall refer to as the angle-of-attack mode, explicit formulas are derived which yield accurate values of the period and damping at all altitudes. The resonance altitude where the two oscillatory

modes have equal periods is obtained by solving a very simple equation. This value for critical altitude is also accurate to within 10 feet of the exact numerical solution.

THE EQUATIONS OF MOTION

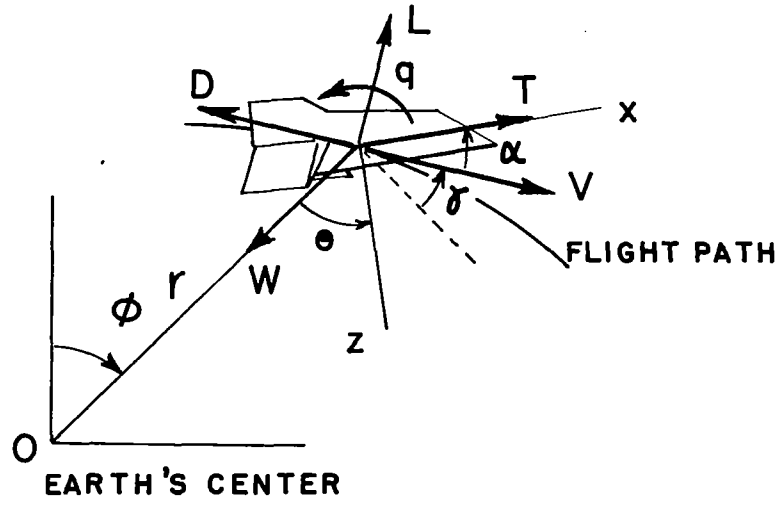

Fig. 1 Axes System and Nomenclature

If we use an axes system that is always tangent to the flight path as shown in Fig. 1, the motion of a lifting vehicle with constant thrust is governed by the system of equations*

$$
\begin{aligned}
\frac{dV}{dt} &= \frac{T}{m}\cos\alpha - \frac{\rho S C_D V^2}{2m} - g\sin\gamma \\
V\frac{d\gamma}{dt} &= \frac{T}{m}\sin\alpha + \frac{\rho S C_L V^2}{2m} - \left(g - \frac{V^2}{r}\right)\cos\gamma \\
\frac{dq}{dt} &= \frac{\rho S L C_m V^2}{2B} - \frac{3}{2}\frac{g}{r}\frac{(A-C)}{B}\sin 2\theta \\
\frac{d\theta}{dt} &= q + \frac{V}{r}\cos\gamma \\
\frac{dr}{dt} &= V\sin\gamma \\
\theta &= \gamma + \alpha
\end{aligned}
\tag{1}
$$

*All symbols are defined in notation section.

The first two equations are, respectively, the drag and lift equations along the tangent and normal to the flight path. The constant thrust, T, is set for a reference circular orbit of radius r_0 with constant lift and drag coefficients. Furthermore, the thrust is small enough that the mass of the vehicle can be assumed constant. Hence, along the reference orbit, where $\gamma = \alpha = 0$

$$T = \tfrac{1}{2}\rho_0 S C_{D_0} u_0^2$$

$$1 - \frac{u_0^2}{g_0 r_0} = \frac{\rho_0 S C_{L_0} u_0^2}{2 m g_0} \qquad (2)$$

$$C_{m_0} = 0$$

$$q_0 = -\frac{u_0}{r_0}$$

The first term on the right-hand-side of the pitching moment equation, Eq. (1-3), expresses the restoring aerodynamic torque, while the second term corresponds to the gravity torque. The last three of Eqs. (1) are kinematic relationships. The mass density, ρ, of the atmosphere is solely altitude dependent. For computational purposes the atmospheric data used were obtained from a polynomial representation of the 1962 U.S. standard atmosphere as presented in the 1966 U.S. standard atmosphere supplements. The lift and drag coefficients, $C_L(\alpha)$ and $C_D(\alpha)$, are functions of the angle-of-attack only, while the pitching moment coefficient $C_m(\alpha, q)$ depends on both the angle-of-attack and the angular velocity in pitch relative to the earth.

To write the equations in non-dimensional forms, let

$$V(t) = u_0 \hat{u}(t), \quad r(t) = r_0 \hat{r}(t), \quad q(t) = \frac{2u_0}{L} \hat{q}(t)$$

$$\rho(r) = \rho_0 \hat{\rho}(r), \quad g(r) = g_0 \left(\frac{r_0}{r}\right)^2 = g_0 \left(\frac{1}{\hat{r}}\right)^2 \qquad (3)$$

Furthermore, to the first order

$$C_D(\alpha) = C_{D_0} + C_{D_\alpha} \alpha$$

$$C_L(\alpha) = C_{L_0} + C_{L_\alpha} \alpha \qquad (4)$$

$$C_m(\alpha, q) = C_{m_0} + C_{m_\alpha}\alpha + \frac{L}{2u_0} C_{m_{\hat{q}}}(q - q_0)$$

where C_{D_0}, C_{L_0} and C_{m_0} are the drag, lift and pitching moment coefficients along the reference flight path.

With the definitions

$$\hat{t} = \frac{g_0}{u_0}t, \quad k_y^2 = \frac{B}{m}, \quad \frac{d}{d\hat{t}}(\ ) = (\dot{\ })$$

$$\mu = \frac{\rho_0 S u_0^2}{2mg_0}, \quad k_0 = \frac{(A - C)}{B}, \quad \eta = \frac{2r_0}{L} \tag{5}$$

$$s^2 = \frac{u_0^2}{g_0 r_0}, \quad \delta = \left(\frac{L}{2k_y}\right)^2$$

the non-dimensional equations of motion can be written as

$$\dot{\hat{u}} = \mu C_{D_0} \cos\alpha - \mu\hat{\rho}\hat{u}^2 C_D(\alpha) - \frac{1}{\hat{r}^2}\sin\gamma$$

$$\hat{u}\dot{\gamma} = \mu C_{D_0} \sin\alpha + \mu\hat{\rho}\hat{u}^2 C_L(\alpha) - \left(\frac{1}{\hat{r}^2} - \frac{s^2\hat{u}^2}{\hat{r}}\right)\cos\gamma \tag{6}$$

$$\dot{\hat{q}} = 2\mu\delta\hat{\rho}\hat{u}^2 C_m(\alpha, \hat{q}) - \frac{3k_0}{2\eta\hat{r}^3}\sin 2\theta$$

$$\dot{\theta} = s^2\eta\hat{q} + s^2\frac{\hat{u}}{\hat{r}}\cos\gamma$$

$$\dot{\hat{r}} = s^2\hat{u}\sin\gamma$$

$$\theta = \gamma + \alpha$$

We see now that, for prescribed initial conditions, integrating the system of Eqs. (6) is a formidable task. The task is eased, however, by decoupling the equations. To this end, we shall assume that the motion of the vehicle around its center of mass has negligible effect on the orbit, that is, on the trajectory mode. This assumption is justified since the vehicle is small in comparison with the dimension of the orbit and since the aerodynamic forces in the altitude range considered are also small. This statement of the so-called limited problem has been used in celestial mechanics to study the

libration of the moon. Based on this decoupling, we shall first calculate the trajectory mode, and then use the results to integrate the equations governing the angle-of-attack oscillations. The coupling effects will be examined in the last part of the paper.

PHUGOID OSCILLATIONS

The phugoid, or long period oscillations, occur at nearly constant angle-of-attack. Hence, by taking $\alpha \approx 0$, we have the non-dimensional equations which govern the phugoid mode.

$$\dot{\hat{u}} = \mu C_{D_0}(1 - \hat{\rho}\hat{u}^2) - \frac{1}{\hat{r}^2}\sin\gamma$$

$$\hat{u}\dot{\gamma} = (1 - s^2)\hat{\rho}\hat{u}^2 - \left(\frac{1}{\hat{r}^2} - \frac{s^2\hat{u}^2}{\hat{r}}\right)\cos\gamma \qquad (7)$$

$$\dot{\hat{r}} = s^2\hat{u}\sin\gamma$$

We note that s is the ratio of the circular velocity to the orbital circular velocity without drag. At very high altitude $s \to 1$ and $\rho \to 0$ and the first and the third of Eqs. (7) reduce to

$$\dot{\hat{u}} = -\frac{1}{\hat{r}^2}\sin\gamma$$

$$\dot{\hat{r}} = \hat{u}\sin\gamma$$

From these, we have the energy integral

$$\frac{1}{2}\hat{u}^2 - \frac{1}{\hat{r}} = \text{constant}$$

In general, the force field is not conservative since the energy is dissipated by atmospheric drag.

If we allow only small departures from the equilibrium flight path, we can express the orbital parameters in terms of small perturbations

$$\hat{u}(\hat{t}) = 1 + \hat{u}_1(\hat{t})$$
$$\hat{r}(\hat{t}) = 1 + \hat{r}_1(\hat{t}) \tag{8}$$
$$\gamma(\hat{t}) = \gamma_1(\hat{t})$$

Also, by expanding the mass density $\hat{\rho}(\hat{r})$ in a Taylor's series in $\hat{r}_1$, we have

$$\hat{\rho}(\hat{r}) = 1 + \sigma_1 \hat{r}_1 + \sigma_2 \hat{r}_1^2 + \cdots \tag{9}$$

where

$$\sigma_1 = \left(\frac{d\rho}{dr}\right)_0 \frac{r_0}{\rho_0}, \quad \sigma_2 = \tfrac{1}{2}\left(\frac{d^2\rho}{dr^2}\right)_0 \frac{r_0^2}{\rho_0}, \quad \cdots \tag{10}$$

Further, let

$$\omega^2 = (1 - s^2)(-\sigma_1 s^2 + 2) + s^4$$
$$\beta = -\tfrac{1}{2}s^2[(1 - s^2)(\sigma_2 - 1) - 2] \tag{11}$$
$$\tau = \omega\hat{t}, \quad \frac{d}{d\tau}(\ ) = (\ )'$$

To the second order of smallness in the perturbations, we can rewrite the system of Eqs. (7) in matrix form

$$X'(\tau) = AX(\tau) + B(X) \tag{12}$$

where

$$X(\tau) = \begin{bmatrix} \hat{u}_1 \\ \gamma_1 \\ \hat{r}_1 \end{bmatrix}, \quad A = \frac{1}{\omega}\begin{bmatrix} -2\mu C_{D_0} & -1 & -\mu C_{D_0}\sigma_1 \\ 2 & 0 & \dfrac{2-\omega^2}{s^2} \\ 0 & s^2 & 0 \end{bmatrix} \tag{13}$$

$$B(X) = \frac{1}{\omega}\begin{bmatrix} -\mu C_{D_0}(\hat{u}_1^2 + 2\sigma_1 \hat{u}_1 \hat{r}_1 + \sigma_2 \hat{r}_1^2) + 2\gamma_1 \hat{r}_1 \\ -\hat{u}_1^2 + \tfrac{1}{2}(1 - s^2)\gamma_1^2 - \dfrac{2\beta}{s^2}\hat{r}_1^2 - \dfrac{1}{s^2}(\omega^2 - 2 + 4s^2)\hat{r}_1 \hat{u}_1 \\ s^2 \hat{u}_1 \gamma_1 \end{bmatrix}$$

Let ϵ be an initial perturbation of any one of the variables, say $\hat{r}_1$. We can then assume series solutions of the form

$$\begin{aligned} \hat{u}_1 &= \epsilon \hat{u}_{11} + \epsilon^2 \hat{u}_{12} + \cdots \\ \gamma_1 &= \epsilon \gamma_{11} + \epsilon^2 \gamma_{12} + \cdots \\ \hat{r}_1 &= \epsilon \hat{r}_{11} + \epsilon^2 \hat{r}_{12} + \cdots \end{aligned} \tag{14}$$

or

$$X = \epsilon X_1 + \epsilon^2 X_2 + \cdots \tag{15}$$

where the definitions of the column vectors X_1, X_2, ... are clear from Eq. (14). By substituting into Eq. (12) and equating coefficients of like powers in ϵ we have the system of differential equations

$$X_1' = AX_1 \tag{16}$$

$$X_2' = AX_2 + B(X_1) \tag{17}$$

Since A is a constant matrix we can immediately integrate Eq. (16) to have

$$X_1(\tau) = e^{A\tau} X_1^0 \tag{18}$$

where

$$X_1^0 = X_1(0) = \frac{1}{\epsilon} X(0) \tag{19}$$

With this value of $X_1(\tau)$ we can express $B(X_1)$ as a function of τ and consider Eq. (17) as a linear system of differential equations with a forcing term. By integrating we have

$$X_2(\tau) = e^{A\tau} X_2^0 + \int_0^\tau e^{A(\tau - t)} B(t)\, dt \tag{20}$$

But

$$X_2^0 = X_2(0) = 0$$

Hence

$$X_2(\tau) = \int_0^\tau e^{A(\tau - t)} B(t)\, dt \tag{21}$$

and the solution to the second order, of the phugoid mode, is

$$X(\tau) = \epsilon e^{A\tau} X_1^0 + \epsilon^2 \int_0^\tau e^{A(\tau - t)} B(t)\, dt \tag{22}$$

Linear Solution

The integration of Eq. (16) gives the linear solution. The system has the characteristic equation

$$\lambda^3 + \frac{2\mu C_{D_0}}{\omega}\lambda^2 + \lambda - \frac{2\mu C_{D_0}}{\omega}\left(\frac{\xi}{\omega}\right)^2 = 0 \tag{23}$$

where

$$\xi^2 = s^2[-(1+\sigma_1)s^2 + 2] = -\omega^2 - \sigma_1 s^2 + 2 \tag{24}$$

In general, the characteristic equation has a pair of complex conjugate roots corresponding to the phugoid oscillations and a real root corresponding to the spiral mode. The last term of the characteristic equation induces the spiral mode and is a small quantity. Let

$$\lambda_{\text{spiral}} = \frac{2\mu C_{D_0}}{\omega}\left(\frac{\xi}{\omega}\right)^2 a \tag{25}$$

where a is a quantity to be determined. By substituting into Eq. (23) we have

$$a = 1 - \left(\frac{2\mu C_{D_0}}{\omega}\right)^2 \left(\frac{\xi}{\omega}\right)^2 a^2 \left(1 + \left(\frac{\xi}{\omega}\right)^2 a\right) \tag{26}$$

Using Lagrange's expansion[3] we have for the value of a

$$\begin{aligned} a = 1 &- \left(\frac{2\mu C_{D_0}}{\omega}\right)^2 \left(\frac{\xi}{\omega}\right)^2 \left(1 + \left(\frac{\xi}{\omega}\right)^2\right) + \left(\frac{2\mu C_{D_0}}{\omega}\right)^4 \left(\frac{\xi}{\omega}\right)^4 \left(1 + \left(\frac{\xi}{\omega}\right)^2\right)\left(2 + 3\left(\frac{\xi}{\omega}\right)^2\right) \\ &- \left(\frac{2\mu C_{D_0}}{\omega}\right)^6 \left(\frac{\xi}{\omega}\right)^6 \left(1 + \left(\frac{\xi}{\omega}\right)^2\right)\left(1 + 2\left(\frac{\xi}{\omega}\right)^2\right)\left(5 + 6\left(\frac{\xi}{\omega}\right)^2\right) + \cdots \end{aligned} \tag{27}$$

Then by factorizing the cubic equations, Eq. (23), we have for the phugoid mode

$$\lambda^2 + \frac{2\mu C_{D_0}}{\omega}\left(1 + \left(\frac{\xi}{\omega}\right)^2 a\right)\lambda + a^{-1} = 0 \tag{28}$$

This gives

$$\text{Real}\,(\lambda_{\text{phugoid}}) = -\frac{\mu C_{D_0}}{\omega}\left(1 + \left(\frac{\xi}{\omega}\right)^2 a\right)$$

$$\text{Im}\,(\lambda_{\text{phugoid}}) = \left[1 - \left(\frac{\mu C_{D_0}}{\omega}\right)^2\left(1 + \left(\frac{\xi}{\omega}\right)^2 a\right)\left(1 - 3\left(\frac{\xi}{\omega}\right)^2 a\right)\right]^{\frac{1}{2}} \tag{29}$$

With the roots calculated we have for the spiral mode in real time

$$t_{\text{double}} = \frac{0.69m}{\rho_0 S C_{D_0} u_0}\left(\frac{\omega}{\xi}\right)^2\left[1 + \left(\frac{2\mu C_{D_0}}{\omega}\right)^2\left(\frac{\xi}{\omega}\right)^2 a\left(1 + \left(\frac{\xi}{\omega}\right)^2 a\right)\right] \tag{30}$$

For the phugoid mode the damping is given by

$$t_{\text{half}} = \frac{1.38m}{\rho_0 S C_{D_0} u_0} \times \frac{1}{1 + \left(\frac{\xi}{\omega}\right)^2 a} \tag{31}$$

In real time, the phugoid period is

$$T = \frac{2\pi u_0}{\omega g_0}\left[1 - \left(\frac{\mu C_{D_0}}{\omega}\right)^2\left(1 + \left(\frac{\xi}{\omega}\right)^2 a\right)\left(1 - 3\left(\frac{\xi}{\omega}\right)^2 a\right)\right]^{-\frac{1}{2}} \tag{32}$$

In the last equation, by taking the bracket equal to unity we have a result that is identical to Laitone and Chou's Eq. $(1.5)^2$. At very high altitudes, ω tends to unity and ρ tends to zero. The phugoid period asymptotically tends to the circular orbital period. In reality, after a perturbation has been applied in a vacuum, the vehicle will go into a slightly elliptical orbit. Thus, T should tend to this elliptic orbital period. This correct orbital period appears only when we consider non-linear terms.

In general, the quantity $\left(\frac{2\mu C_{D_0}}{\omega}\right)^2\left(\frac{\xi}{\omega}\right)^2$ in the expansion of a, Eq. (27), is small and setting a = 1 gives a very good approximation. This expansion gives the roots of the characteristic equation explicitly to the desired degree of accuracy. In our derivation, the damping term for the phugoid is

$$\exp\left[-\frac{\rho_0 u_0 S C_{D_0}}{2m}\left(1 + \left(\frac{\xi}{\omega}\right)^2 a\right)t\right] \tag{33}$$

where a is explicitly given by the series expansion, Eq. (27). Using a = 1 we have Laitone and Chou's Eq. (3.9) for phugoid damping. Hence, besides the additional spiral mode obtained, the above results greatly improve the already accurate formulas for phugoid oscillations derived in Ref. 2.

Now let

$$\lambda_{\text{phugoid}} = \lambda_1 \pm i\omega_1 \tag{34}$$

$$\lambda_{\text{spiral}} = \lambda_2$$

With the roots calculated, we have, to the first order, for the elements of the flight path

$$\hat{r} = 1 + \epsilon C_1 e^{\lambda_2 \tau} + \epsilon e^{\lambda_1 \tau}[C_2 \cos\omega_1\tau + C_3 \sin\omega_1\tau]$$

$$\gamma = \frac{\epsilon\omega\lambda_2}{s^2} C_1 e^{\lambda_2\tau} + \epsilon\frac{\omega}{s^2} e^{\lambda_1\tau}[(\omega_1 C_3 + \lambda_1 C_2)\cos\omega_1\tau - (\omega_1 C_2 - \lambda_1 C_3)\sin\omega_1\tau]$$

$$\hat{u} = 1 + \frac{\epsilon}{2s^2}[(\omega^2 - 2) + \omega^2\lambda_2^2]C_1 e^{\lambda_2\tau} \tag{35}$$

$$+ \frac{\epsilon}{2s^2} e^{\lambda_1\tau}\left\{\left[[(\omega^2 - 2) + \omega^2(\lambda_1^2 - \omega_1^2)]C_2 + 2\omega^2\omega_1\lambda_1 C_3\right]\cos\omega_1\tau\right.$$

$$\left. + \left[[(\omega^2 - 2) + \omega^2(\lambda_1^2 - \omega_1^2)]C_3 - 2\omega^2\omega_1\lambda_1 C_2\right]\sin\omega_1\tau\right\}$$

where the C_i are constants of integration.

From these expressions we have the following interesting remarks:

1. In each of the variations of elements such as radial distance, flight path angle, and velocity, there are two components. One component is oscillatory with diminishing amplitude and it tends to circularize the flight path. The other component is aperiodic and divergent. This component is due to the offset effect between the thrust and the drag and induces a secular variation of the elements of the orbit.

2. For the vehicle considered in Ref. 1, $\omega_1 > 1$ above about 140,000 ft, and $\omega_1 \to 1$ as $r_0 \to \infty$, thus the effect of drag is to shorten the phugoid period.

3. In the expression for $\hat{r}$, since $\lambda_2 > 0$, the divergent mode tends to decrease the radial distance if the initial perturbations are such that $\epsilon C_1 < 0$. On the contrary if $\epsilon C_1 > 0$ the radial distance will increase with time. Furthermore, under the constant thrust application, with decreasing drag, the vehicle will move outward following a spiral.

4. From the expression for the flight path angle we can see that it varies in the same direction as the radial distance.

5. On the contrary, the velocity varies as the radial distance if and only if

$$\omega^2 > \frac{2}{1+\lambda_2^2} \tag{36}$$

If the inequality is satisfied the velocity will increase as the vehicle is spiraling out and decrease if the vehicle is spiraling in. The inverse is true if the inequality reverses. To calculate the altitude where the velocity inversion occurs, since λ_2^2 is small, we can use the equation

$$\omega^2 = 2 \tag{37}$$

The Eqs. (35) are derived in terms of the non-dimensional time τ, and the frequency of oscillations ω_1 is given by Eq. (29). In terms of the non-dimensional time, $\hat{t}$, the frequency of oscillations is $\omega_1\omega$ which can be approximated by ω since ω_1 is near unity. The square of the linear phugoid frequency, ω^2, is plotted versus the altitude in Fig. 2.

We see that ω^2 is large at low altitudes and tends asymptotically to 1 when the altitude increases indefinitely. When $\omega^2 = 2$ the velocity inversion occurs. More explicitly, using the definition in Eqs. (11) for ω^2, we have

$$\frac{(W/S)_s}{C_{L_0}} = -\frac{g_s r_0}{2}(2\rho_0 + \rho_0' r_0) \tag{38}$$

where subscript, s, denotes the condition at sea level and ρ_0' is the density gradient evaluated at r_0. The left-hand side of the formula above is a characteristic of the vehicle and the right-hand side is solely dependent on the characteristic of the atmosphere. Fig. 3 is a plot of Eq. (38) as a function of the altitude and the graph can be used to determine the altitude where the velocity inversion occurs for any given vehicle. For example, the vehicle considered in Ref. 1 has $(W/S)_s/C_{L_0} = 600$ lb/ft.^{2} Thus, the critical altitude for velocity inversion is 321,000 ft.

Eq. (38) gives the critical altitude to within 10 ft. of the value computed numerically from the exact linear equations.

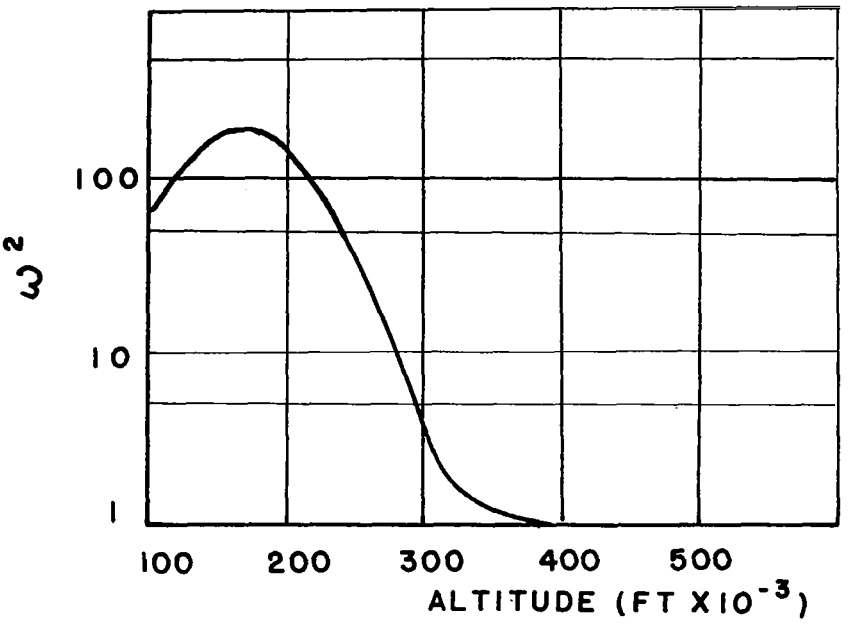

Fig. 2. Linear Phugoid Frequency

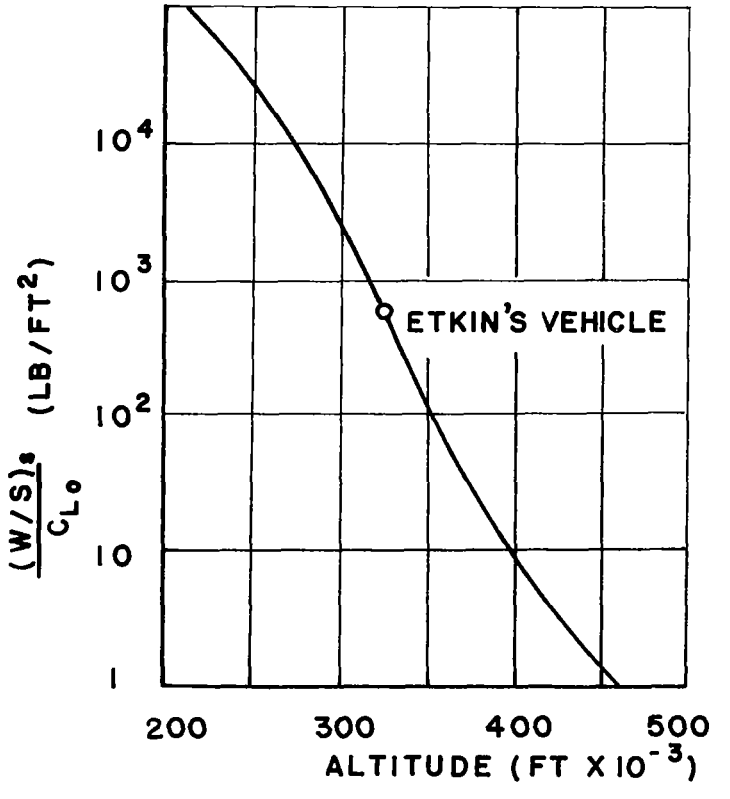

Fig. 3. Speed Perturbation Inversion Altitude

Non-Linear Solution

We have seen that the next higher order component of the vector state is $\epsilon^2 X_2$. If $B(t) \equiv B(X_1)$, then

$$X_2 = \int_0^\tau e^{A(\tau - t)} B(t)\, dt \tag{39}$$

and, A and B are given by Eq. (13) and X_1 represents the linear solution found in the preceding section. Hence the computation of $X_2(\tau)$ is straightforward. Here we need only to have an idea of the order of magnitude of the second order term. By the form of the vector $B(X_1)$, we can see that, if the perturbation is small, the contribution of $\epsilon^2 X_2$ is negligible. This has been shown in a numerical study by Rangi.[4] But in the expansion, Eq. (9), of the mass density of the atmosphere, σ_2 is of the order 10^5. Hence, if $\epsilon > 0(10^{-4})$ we should include the second order gradient effect of the air mass density σ_2 which appears explicitly in $B(X_1)$. By the same consideration, terms which need to be retained in B are

$$B(X_1) = \begin{bmatrix} -\frac{\mu C_{D_0}}{\omega} \sigma_2 \hat{r}_{11}^2 \\ -\frac{2\beta}{s^2 \omega} \hat{r}_{11}^2 \\ 0 \end{bmatrix} \tag{40}$$

Hence, the non-linear numerical analysis of Ref. 4 is not valid for large perturbations, since the author has neglected all second and higher order terms of the air mass density. For large perturbations, as were considered in Ref. 4, the prime contributing non-linear factor in the phugoid and spiral trajectory is the variation of the mass density of the atmosphere. The perturbed trajectories for these cases are highly eccentric orbits and it is not correct to assume a linear variation for the air mass density. (See Appendix C)

The value of σ_2 considered above is somewhat too large because of an inverse polynomial representation of the atmospheric mass density. This resulted from a curve fitting analysis which can give a wrong value for a truncated

series at a certain altitude. In trajectory analysis a better approximation is usually found using an exponential atmosphere. However, this atmosphere is not suitable for a dynamics stability analysis in which a series expansion of the air mass density is required.

In this paper, we just want to call attention to the effect of the second order atmospheric gradient. For an accurate second order analysis, the coefficients σ_1 and σ_2 in the "parabolic representation" of $\overset{\curvearrowleft}{\rho}$, Eq. 9, should be averaged for each limited altitude range considered.

Asymptotic Behavior of Phugoid Period

To the first order we have seen that the phugoid period tends to the circular orbital period when the altitude of flight increases indefinitely. In reality, the phugoid period tends to the perturbed elliptical period. To find this correct orbital behavior we use a new time variable, $\bar{t}$, such that

$$\bar{t} = \tau(1 + h_1\epsilon + h_2\epsilon^2 + \cdots)^{-1}$$

where h_1, h_2 are constants to be determined. By substituting into Eq. (39), neglecting drag terms, and requiring a periodic solution for X_2, we can easily find that

$$-h_1 = \frac{(\omega^2 - 2)^2 - 2(1 - s^2)(\omega^2 - 2) + 4s^2(\beta - 2)}{s^2\omega^4} \tag{41}$$

Hence, to the first order, an asymptotic expression for the phugoid period is

$$T = \frac{2\pi u_0}{\omega g_0}(1 + \epsilon h_1 + \cdots) \tag{42}$$

ANGLE OF ATTACK OSCILLATIONS

The angle-of-attack mode is governed by the system

$$\frac{dq}{dt} = \frac{\rho V^2 S L C_m(\alpha, q)}{2B} - \frac{3g(r)}{2r}\frac{(A - C)}{B}\sin 2\theta$$

$$\frac{d\theta}{dt} = q + \frac{V}{r}\cos\gamma \tag{43}$$

$$\theta = \gamma + \alpha$$

The elimination of θ and q results in a non-linear equation in α

$$\frac{d^2\alpha}{dt^2} + \frac{T\cos\alpha}{mV}\frac{d\alpha}{dt} + \frac{\rho SV}{2m}\frac{dC_L(\alpha)}{dt} + \frac{3g}{2r}\frac{(A-C)}{B}\cos 2\gamma \sin 2\alpha$$
$$+ \frac{3g}{2r}\frac{(A-C)}{B}\sin 2\gamma \cos 2\alpha + \frac{T}{m}\frac{\rho S}{2m}(C_L(\alpha)\cos\alpha + C_D(\alpha)\sin\alpha)$$
$$+ \frac{T}{m}\frac{g}{V^2}(2\sin\gamma\sin\alpha + \cos\gamma\cos\alpha) - \left(\frac{T}{m}\right)^2\frac{\sin 2\alpha}{2V^2} \qquad (44)$$
$$- \left(\frac{\rho S}{2m}\right)^2 C_D(\alpha)C_L(\alpha)V^2 - \frac{\rho SC_D(\alpha)}{2m}\, g\cos\gamma$$
$$- \frac{\rho SV^2 L}{2B}C_m(\alpha, q) + \frac{3g}{2r}\sin 2\gamma + \frac{SC_L V}{2m}\frac{d\rho}{dt} - \frac{g^2}{V^2}\sin 2\gamma = 0$$

Linear Solution

A zero-order solution can be obtained easily by considering small oscillations of the angle-of-attack along a circular orbit. Assume

$$\alpha << 1,\ \gamma = 0,\ \frac{d\gamma}{dt} = 0,\ V = u_0,\ r = r_0 \qquad (45)$$

Then Eq. (44) reduces to the linear equation with the non-dimensional time, τ, as the independent variable

$$\alpha'' + \frac{\mu}{\omega}(C_{D_0} + C_{L_\alpha} - 2\delta C_{m_{\hat{q}}})\alpha' + \frac{s^2}{\omega^2}(3k_0 - 2\mu\eta\delta C_{m_\alpha})\alpha = 0 \qquad (46)$$

To the order μ, we have for the angle-of-attack mode

$$\lambda = -\frac{\mu C_{N_1}}{\omega} \pm i\frac{n}{\omega} \qquad (47)$$

where

$$C_{N_1} = \tfrac{1}{2}(C_{D_0} + C_{L_\alpha} - 2\delta C_{m_{\hat{q}}})$$
$$n^2 = s^2(3k_0 - 2\mu\eta\delta C_{m_\alpha}) \qquad (48)$$

The solution, Eq. (47), is identical to Laitone and Chou's result[2] and is in good agreement with the results of the numerical study in Ref. 1.

Explicitly, in real time, the angle-of-attack period is

$$T = \frac{2\pi u_0}{g_0 s}\left[3k_0 - 2\mu\eta\delta C_{m_\alpha}\right]^{-\frac{1}{2}} \tag{49}$$

and the damping is given by

$$\exp\left[-\frac{\mu g_0}{2u_0}(C_{D_0} + C_{L_\alpha} - 2\delta C_{m_{\hat{q}}})t\right] \tag{50}$$

Resonance Altitude

For practical values of vehicle parameters, there is an altitude where the two frequencies, ω and n, can be equal. This altitude, called the resonance altitude, is found by solving the equation $\omega = n$, and for simplicity, setting $s^2 = 1$.

Explicitly, we have

$$\frac{2k_y^2\ (3k_0 - 1)(W/S)_s}{LC_{m_\alpha}} = \rho_0 r_0^2 g_s \tag{51}$$

where subscript s denotes the condition at sea level. The left-hand side of the formula above is a characteristic of the vehicle and the right-hand side is solely dependent on the characteristic of the atmosphere. Fig. 4 presents the variation for the earth's atmosphere as a function of the altitude and the graph can be used to determine the resonance altitude for any given vehicle. For example, for the vehicle considered in Ref. 1, the characteristic value on the left-hand side of Eq. (51) is 5.2281×10^4 lb/ft^3 and the resonance altitude is therefore 492,300 ft. The value of the resonance altitude computed from Eq. (51) is correct to within 10 ft compared with the exact value from a numerical analysis using Etkin's equations.

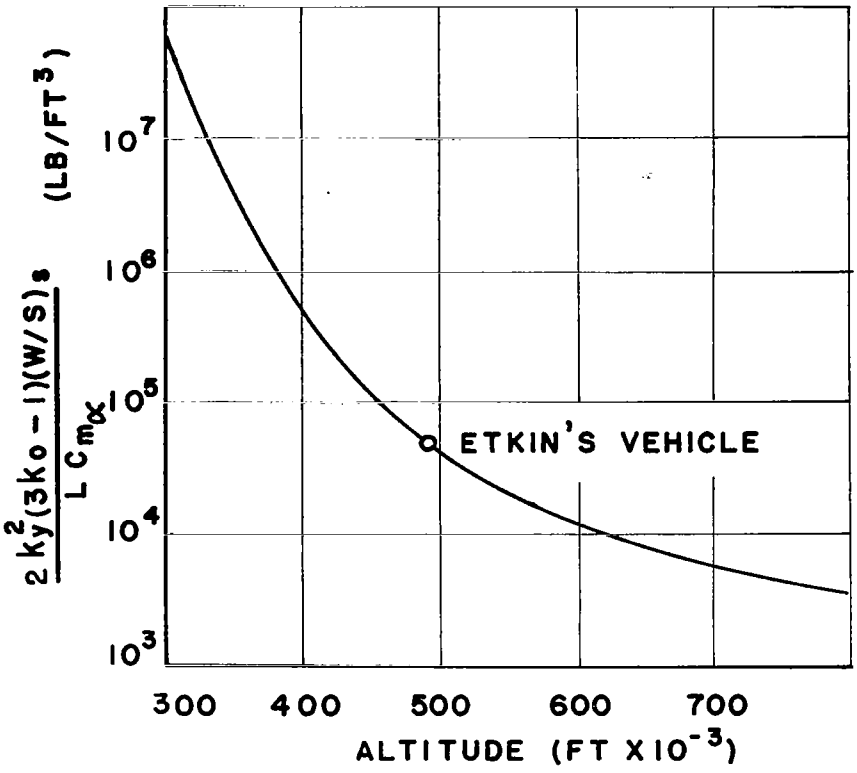

Fig. 4. Resonance Altitude

Coupling Effects

We have assumed that the coupling effects between the two oscillatory modes are negligible. This is, in general, true, below and above the resonance altitude. However, near the resonance altitude, strong coupling effects are evident and the linear solutions, Eqs. (29) and (47), are no longer valid.

In his study[1], Etkin found that the Phugoid period increased with altitude, tending asymptotically to the orbital period. He also found that, for his vehicle, the period of the angle-of-attack mode increased with altitude and crossed over the Phugoid period at about 490, 000 ft, tending asymptotically to infinity at about 505, 000 ft. This behavior is also predicted by the uncoupled oscillatory mode frequencies, Eqs. (29) and (47), and agrees with one's physical intuition. However, a close inspection of the region near the

resonance altitude, using Etkin's linear equations, shows that this description of the behavior of the mode periods is in error and reveals, instead, the phenomenon shown in Fig. 5. There is, in fact, a "switching" of the modes of oscillation at the resonance altitude instead of a "crossing"!

The uncoupled damping constants in Eqs. (29) and (47) show that they will remain negative at all altitudes. However, Fig. 6 shows that near the resonance altitude the Phugoid damping constant becomes positive while the angle-of-attack mode damping constant remains negative. Above the resonance altitude the "switched" angle-of-attack mode damping constant is positive while that of the "switched" Phugoid is negative.

A factorization of the fifth-order characteristic equation, of the linearized coupled equation of motion, that takes into account the effects described above, has been obtained by Dobrzelecki.[5] He found that for the damping constants

$$\text{Real}\,(\lambda_{\text{phugoid}}) = -\left[\frac{\mu C_{D_0}}{\omega}\left(1 + \left(\frac{\xi}{\omega}\right)^2 a\right) - K\frac{\mu}{4\omega}(C_{N_1} + C_{N_2})\right] \tag{52}$$

$$\text{Real}\,(\lambda_{\text{attack}}) = -\left[\frac{\mu C_{N_1}}{\omega} + K\frac{\mu}{4\omega}(C_{N_1} + C_{N_2})\right] \tag{53}$$

where

$$K = \frac{2[s^2(1+s^2) + 3k_0 s^2 - \omega^2]}{\omega^2\left[1 - \left(\frac{n}{\omega}\right)^2\right]}$$

$$C_{N_2} = \tfrac{1}{2}[C_{D_0} + C_{L_\alpha} + 2\delta C_{m_{\hat{q}}}] \tag{54}$$

and the coupling coefficient K is positive below and negative above the resonance altitude.

Eqs. (52) and (53), together with the equations for ω and n, correctly and accurately predict the values of the damping constants and frequencies of the oscillatory modes, to within a few thousand feet below and above the

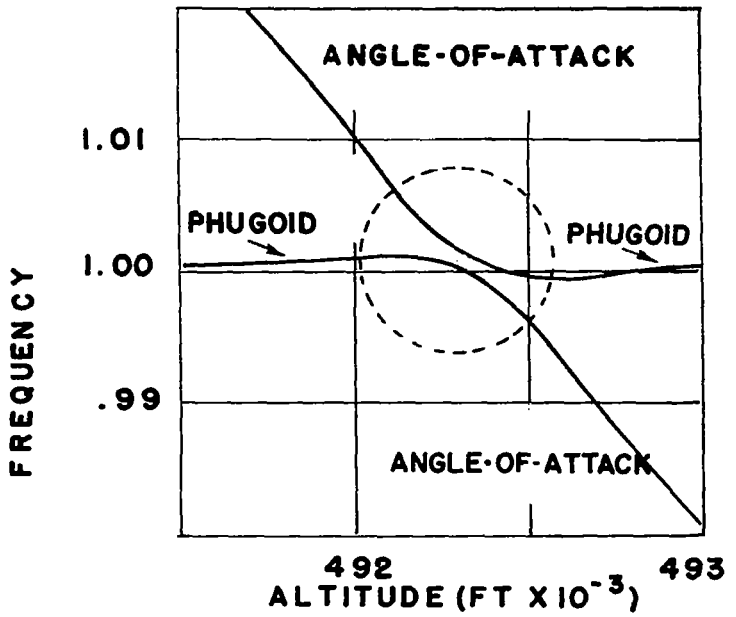

Fig. 5. Frequencies Near Resonance Altitude

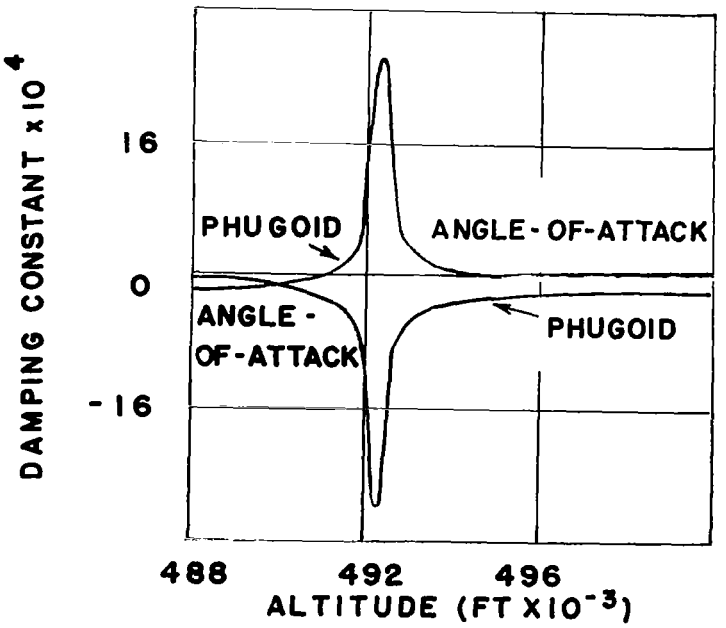

Fig. 6. Damping Constants Near Resonance Altitude

resonance altitude. Figs. 5 and 6 clearly show that near the resonance altitude one has to consider the non-linear equations of motion to predict correctly the crossing of the periods.

Non-Linear Angle-of-Attack Frequency

At high altitudes, especially near the resonance altitude, the amplitude of oscillation of the angle-of-attack may be large. The mode is governed by the non-linear Eq. (44). A simplification may be made by observing that the aerodynamic forces are small and, thus, we can consider the orbit as an exact Keplerian ellipse for the duration of one or several revolutions. Furthermore, by considering a circular orbit and neglecting quantities of the order μ^2 and the negligible damping, we have an equation with τ as the independent variable.

$$\alpha'' + \frac{3s^2 k_0}{\omega^2} \sin\alpha \cos\alpha - \frac{2\mu s^2 \eta\delta}{\omega^2} C_m = 0 \tag{55}$$

This non-linear equation is similar to the equation derived by V. V. Beletskii (Ref. 6, p. 72) with one difference. Here we have a constant low thrust while Beletskii explicitly assumed a drag-free orbital period for the trajectory.

For a slender vehicle with a conical surface of attack, an approximate expression for the pitching moment coefficient is

$$C_m = \overline{C}_{m_\alpha} \sin\alpha \cos\alpha \tag{56}$$

where $\overline{C}_{m_\alpha} \approx C_{m_\alpha}$ can be evaluated by using the simple Newtonian impact theory for moderate angle-of-attack. Accurate values for $\overline{C}_{m_\alpha}$ can be obtained from wind-tunnel measurements. With this assumption, the non-linear equation for the angle-of-attack is

$$\alpha'' + \frac{\overline{n}^2}{\omega^2} \sin\alpha \cos\alpha = 0 \tag{57}$$

where

$$\overline{n}^2 = s^2(3k_0 - 2\mu\eta\delta\overline{C}_{m_\alpha}) \approx n^2 \tag{58}$$

Eq. (57) can be integrated easily using the theory of elliptic integrals or the so-called Lindstedt method for obtaining periodic solutions to non-linear equations (Ref. 7, p. 141). The period of oscillation for large angle-of-attack obtained, in real time, is

$$T = \frac{2\pi u_0}{g_0 s}(3k_0 - 2\mu\eta\delta\bar{C}_{m_\alpha})(1 + \frac{1}{4}\alpha_0^2 + \frac{11}{192}\alpha_0^4 + \cdots) \tag{59}$$

where α_0 is the initial perturbed angle of attack. We notice that resonance does not appear for circular orbits.

Eccentricity Oscillations

If the orbit is elliptical, the result is qualitatively different since the coefficients of the non-linear equation are periodic quantities. The most significant effect is the forced oscillations due to the non-vanishing eccentricity of the orbit. This effect will give rise to a possible resonance. Let us consider a slightly perturbed Keplerian ellipse about the reference circular orbit, then

$$r = \frac{r_0(1 - \epsilon^2)}{1 + \epsilon\cos\tau} \tag{60}$$

where ϵ is small. To the order ϵ we have

$$\begin{aligned} &r = r_0(1 - \epsilon\cos\tau), \quad V^2 = g_0 r_0 (1 + 2\epsilon\cos\tau) \\ &V = (g_0 r_0)^{\frac{1}{2}}(1 + \epsilon\cos\tau), \quad g = g_0(1 + 2\epsilon\cos\tau) \\ &\sin\gamma = \frac{\omega}{s}\epsilon\sin\tau, \quad \cos\gamma = \frac{\omega}{s}(1 - 2\epsilon\cos\tau) \\ &\rho = \rho_0(1 - \epsilon\sigma_1\cos\tau), \quad \tau = \frac{g_0\omega}{u_0}t \end{aligned} \tag{61}$$

Neglecting both damping and quantities of order μ^2, and taking $\omega = s = 1$, we have

$$\begin{aligned} &\alpha'' + [(3k_0 - 2\mu\eta\delta\bar{C}_{m_\alpha}) - \epsilon(3k_0 - 2(\sigma_1 - 2)\mu\eta\delta\bar{C}_{m_\alpha})\cos\tau]\sin\alpha\cos\alpha \\ &\quad + 3\epsilon k_0 \sin\tau\cos 2\alpha + \mu C_{D_0}\cos\alpha \\ &\quad = \mu C_{D_0}(1 - \epsilon\sigma_1\cos\tau) - \epsilon\sin\tau - \mu C_{L_0}\sigma_1\epsilon\sin\tau \end{aligned} \tag{62}$$

To display the effect of eccentricity oscillations, let us consider the case of small angle-of-attack. This gives us a Mathieu equation with forcing terms

$$\alpha'' + (a^2 - \epsilon b \cos\tau)\alpha = -\epsilon(c \sin\tau + d \cos\tau) \tag{63}$$

where

$$\begin{aligned} a^2 &= 3k_0 - 2\mu\eta\delta\bar{C}_{m_\alpha} \\ b &= 3k_0 - 2(\sigma_1 - 2)\mu\eta\delta\bar{C}_{m_\alpha} \\ c &= 3k_0 + 1 + \mu C_{L_0}\sigma_1 \\ d &= \mu C_{D_0}\sigma_1 \end{aligned} \tag{64}$$

The homogeneous Mathieu equations have a periodic solution which can be obtained with classical methods. Here we seek a particular solution for the non-homogeneous Eq. (63) with each of the two forcing functions. For example, consider

$$\alpha'' + (a^2 - \epsilon b \cos\tau)\alpha = -\epsilon c \sin\tau \tag{65}$$

and assume a particular solution of the form

$$\alpha_e = -\epsilon c \sin\tau\phi(\tau) \tag{66}$$

By substituting into Eq. (65) we have an equation for ϕ

$$(1 - x^2)\frac{d^2\phi}{dx^2} - 3x\frac{d\phi}{dx} + (a^2 - 1 - \epsilon bx)\phi = 1 \tag{67}$$

where

$$x = \cos\tau \tag{68}$$

A particular solution of Eq. (67) is sought as a series in terms of the small parameter ϵ. Let

$$\phi(x) = \phi_0 + \epsilon\phi_1 + \epsilon^2\phi_2 + \cdots \tag{69}$$

Then by substituting into Eq. (67) and equating terms of the same order of magnitude we have

$$(1-x^2)\phi_0'' - 3x\phi_0' + (a^2-1)\phi_0 = 1$$
$$(1-x^2)\phi_1'' - 3x\phi_1' + (a^2-1)\phi_1 = bx\phi_0 \qquad (70)$$
$$\cdots$$

where the prime here denotes differentiation with respect to $x = \cos\tau$. The system can be readily integrated to give

$$\phi_0 = \frac{1}{a^2-1}$$
$$\phi_1 = \frac{b\cos\tau}{(a^2-1)(a^2-4)}, \quad \cdots \qquad (71)$$

It is clear that we can do the same with the forcing term $-\epsilon d\cos\tau$, and we have a particular solution for the non-homogeneous Eq. (63). By neglecting $\epsilon^2 d$ we have for a particular solution of Eq. (63)

$$\alpha_e = -\frac{\epsilon}{(a^2-1)}[c\sin\tau + d\cos\tau] - \frac{\epsilon^2 bc\sin 2\tau}{2(a^2-1)(a^2-4)} \qquad (72)$$

In the last expression we can see that $a^2 = 1$ corresponds to a resonance. Our results constitute an extension of Beletskii's study of small eccentric oscillations of a satellite under pure gravity torque (Ref. 6, p. 41). The general solution of Eq. (63) is then the sum of the general solution of the Mathieu equation and the particular integral, Eq. (72).

CONCLUSION

In this paper we have presented an analytical study of the longitudinal dynamics of a thrusting, lifting, orbital vehicle in a nearly circular orbit. Explicit expressions for the elements of the orbit were derived and the behaviors of the variations of these elements were correctly predicted. It was shown that for large perturbations the second order gradient effect of the air mass density must be included. Explicit expressions for the period and damping of the angle-of-attack mode were derived. It was shown that a resonance effect was not present for a circular orbit. A resonance effect was displayed by a study of the forced eccentricity oscillations and the critical altitude for resonance was obtained by solving a very simple equation. The analytical expressions are in excellent agreement with an independent numerical analysis at all altitudes.

REFERENCES

1. B. Etkin, "Longitudinal Dynamics of a Lifting Vehicle in Orbital Flight," J. Aerospace Sci., vol. 28, October 1961, pp. 779-788
2. E. V. Laitone and Y. S. Chou, "Phugoid Oscillations at Hypersonic Speeds," AIAA Journal, vol. 3, April 1965, pp. 732-735
3. R. Bellman, Perturbation Techniques in Mathematics, Physics, and Engineering, Holt, Rinehart and Winston, Inc., New York 1964
4. R. S. Rangi, Non-Linear Effects in the Longitudinal Dynamics of a Lifting Vehicle in Orbital Flight, Univ. of Toronto, UTIA TN 40, October 1960
5. A. Dobrzelecki, Non-Linear Longitudinal Dynamics of A Thrusting, Lifting Orbital Vehicle, Ph.D. Thesis, Univ. of Colorado, 1969
6. V. V. Beletskii, Motion of An Artificial Satellite About Its Center of Mass, NASA Translation, NASA TT F-429, 1966
7. I. G. Malkin, Theory of Stability of Motion, AEC Translation, AEC-TR-3352

APPENDIX A

Characteristics of the Atmosphere

All numerical computations are based on the U.S. Standard Atmosphere, 1962*. However, for ease of computation the approximate inverse polynomial representation of this atmosphere that appears in the U.S. Standard Atmosphere Supplements, 1966†, is assumed to be exact.

The inverse polynomial is of the form

$$\rho/\rho_S = 1/[A_0 + A_1 Z + \cdots + A_{11} Z^{11}]^4 \qquad (A-1)$$

where Z is the geometric altitude above the standard geoid (6378.17 km radius) in kilometers. The coefficients A_j are given in Table A-1.

The polynomial approximation is valid for the altitude range 0-200 km. Compared to the Standard Atmosphere, the approximation differs by less than 5% (see Fig. A-1) in this altitude range.

Fig. A-1 Error in Representing "62" Standard Atmos. By Polynomial Representation. ‡

The non-dimensional density gradients defined in Eq. (10) of the text are plotted in Fig. A-2. For comparison the first density gradient

*U.S. Standard Atmosphere, 1962, prepared under sponsorship of ESSA, NASA, and USAF.

†U.S. Standard Atmosphere Supplements, 1966, prepared under sponsorship of NASA, USAF and U.S. Weather Bureau.

Both publications are available from the Superintendent of Documents, U.S. Government Printing Office, Washington, D.C. 20402.

‡Ibid., p. 68.

(σ_1) obtained by numerical differentiation of the tabulated Standard Atmosphere data is included in the figure.

Table A-1

COEFFICIENTS FOR DENSITY POLYNOMIAL

Altitude range 0-200 km

ρ_s = 1.2250 Kilograms/m^3 A_j [≡] km^j

j	A_j	
0	0.1000000000	E 01
1	0.3393495800	E-01
2	-0.3433553057	E-02
3	0.5497466428	E-03
4	-0.3228358326	E-04
5	0.1106617734	E-05
6	-0.2291755793	E-07
7	0.2902146443	E-09
8	-0.2230070938	E-11
9	0.1010575266	E-13
10	-0.2482089627	E-16
11	0.2548769715	E-19

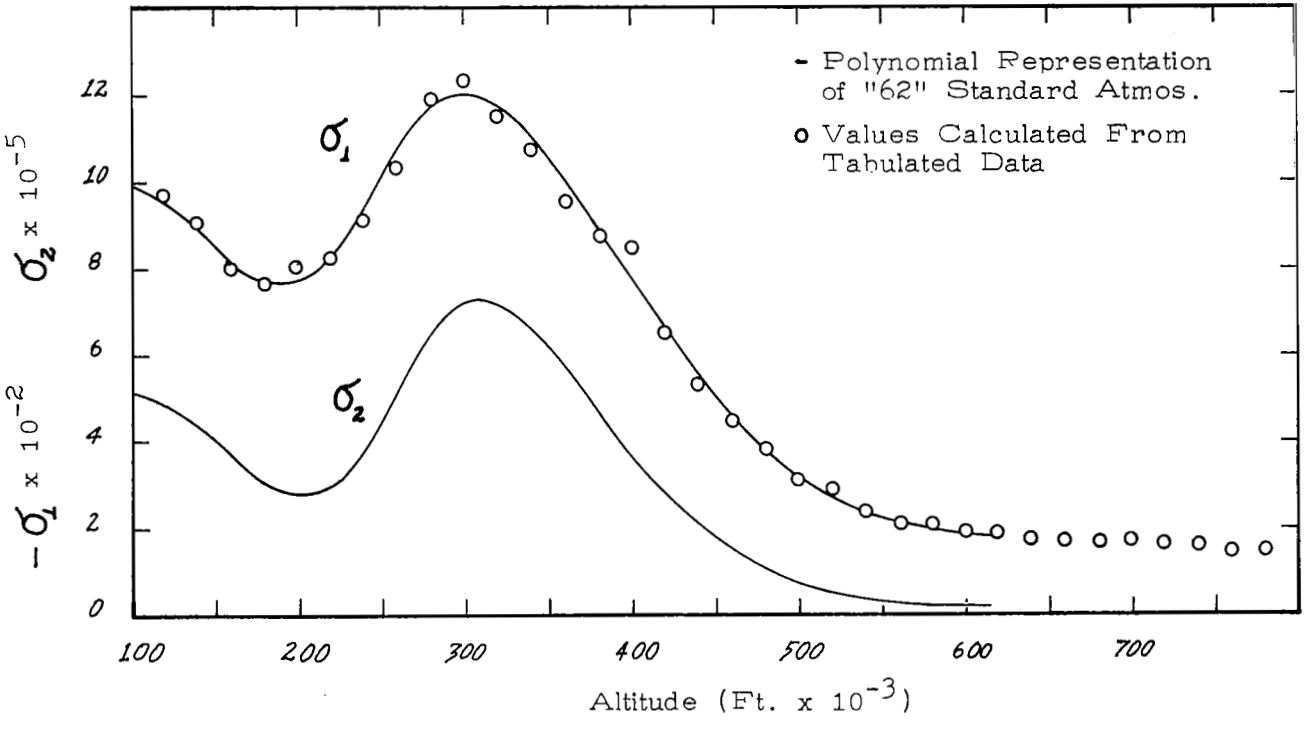

Fig. A-2 Non-Dimensional Density Gradients

APPENDIX B

Characteristic of the Vehicle

The characteristics of the vehicle geometry and the aerodynamic stability derivatives used in all numerical calculations are those used by Etkin[1] and Rangi[4] and are typical for a slender body, a cone or wedge of 3° semiangle. The values were derived from the simple Newtonian impact theory for moderate angles of attack. They are tabulated below.

Table B-1

GEOMETRIC VEHICLE PARAMETERS

$k_y = 6$ ft.	$L = 50$ ft.
$k_0 = -0.94$	$W/S = 30$ psf. (sea level)

Table B-2

AERODYNAMIC STABILITY DERIVATIVES

$$C_{L_0} = 0.05 \qquad C_{D_0} = 0.0133 \qquad C_{m_{\hat{q}}} = \frac{\partial C_m}{\partial(\frac{L}{2u_0} q)} = -0.028$$

$$C_{L_\alpha} = \frac{\partial C_L}{\partial \alpha} = 0.329 \qquad C_{D_\alpha} = \frac{\partial C_D}{\partial \alpha} = 0.15 \qquad C_{m_\alpha} = \frac{\partial C_m}{\partial \alpha} = -0.0548$$

APPENDIX C

Effects of Second Order Atmospheric Mass Density Gradient

In pages 13 and 14 we have discussed the need for inclusion of the second order atmospheric mass density gradient (terms containing σ_2) for an accurate analysis. This effect can be dramatically illustrated by a numerical analysis.

Figures C-1 and C-2 respectively represent the variations of the radial distance and the flight path angle as the time varies. They are reproductions of computer generated plots with different atmospheric mass density laws. The set is generated at an altitude of 300,000 ft, where the density gradients are the largets, with an initial non-dimensional speed decrease of $10^{-3}(\epsilon = \Delta\hat{u} = -10^{-3})$. This corresponds to a perturbation of 25 ft/sec. The equations used are the uncoupled phugoid equations (Eqs. 7, p. 5). The solid lines represent the time histories of the elements of the orbit obtained by a numerical integration of the uncoupled non-linear equations, Eqs. 7. One curve is generated with the exact density law, that is the 44th degree inverse polynomial representation of the 62 Standard Atmosphere. Another curve is obtained by keeping only the second order gradient term. The dotted line represents the linear analytical solutions of the uncoupled motion (Eq. 18) with the value for a to the order μ^8. For comparison the numerical solutions using Etkin's linearized and coupled equations are also plotted. It is clear from the graphs that our linear analytical solutions and Etkin's linear numerical solutions are nearly identical. But they do not compare well after 1/4 of a revolution with the exact solution using the exact atmospheric mass density law. The result can be improved by including higher order density gradients. This is obtained by using our second order solution (Eq. 22). The discrepancies are much less at higher altitude where atmospheric drag is small and at lower altitude where the period is short and practical perturbations are small. The time scale taken for the plots

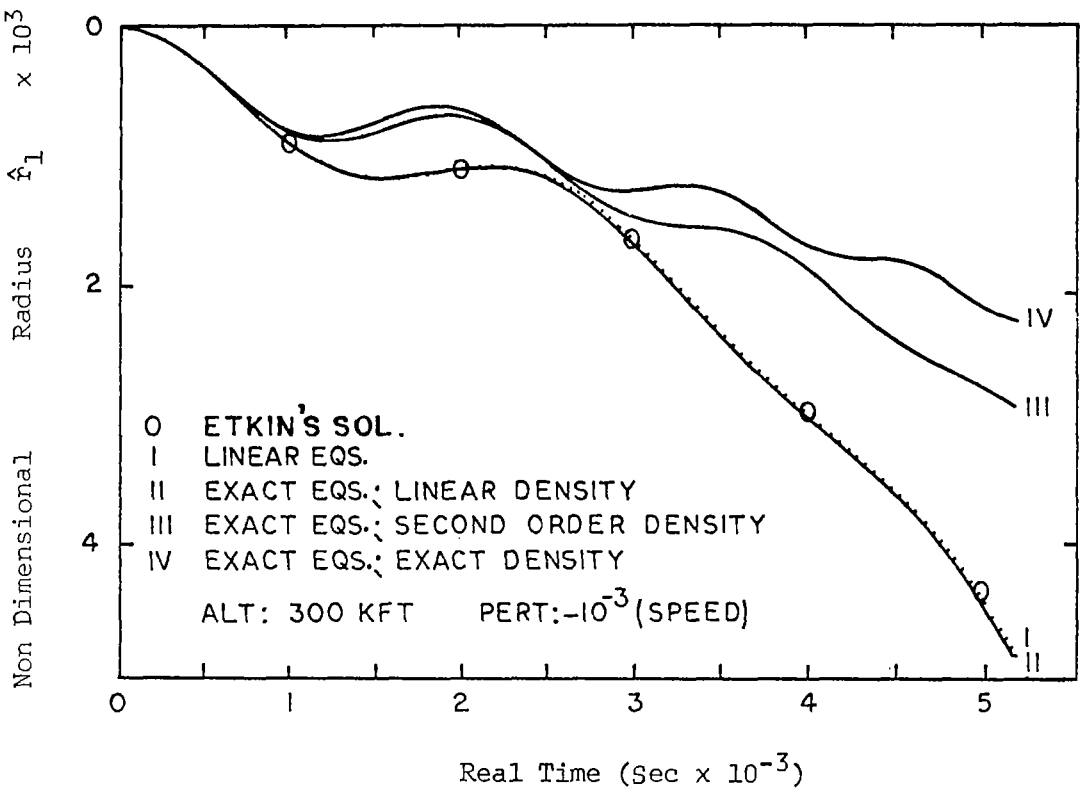

Fig. C-1 Variations of Radial Distance

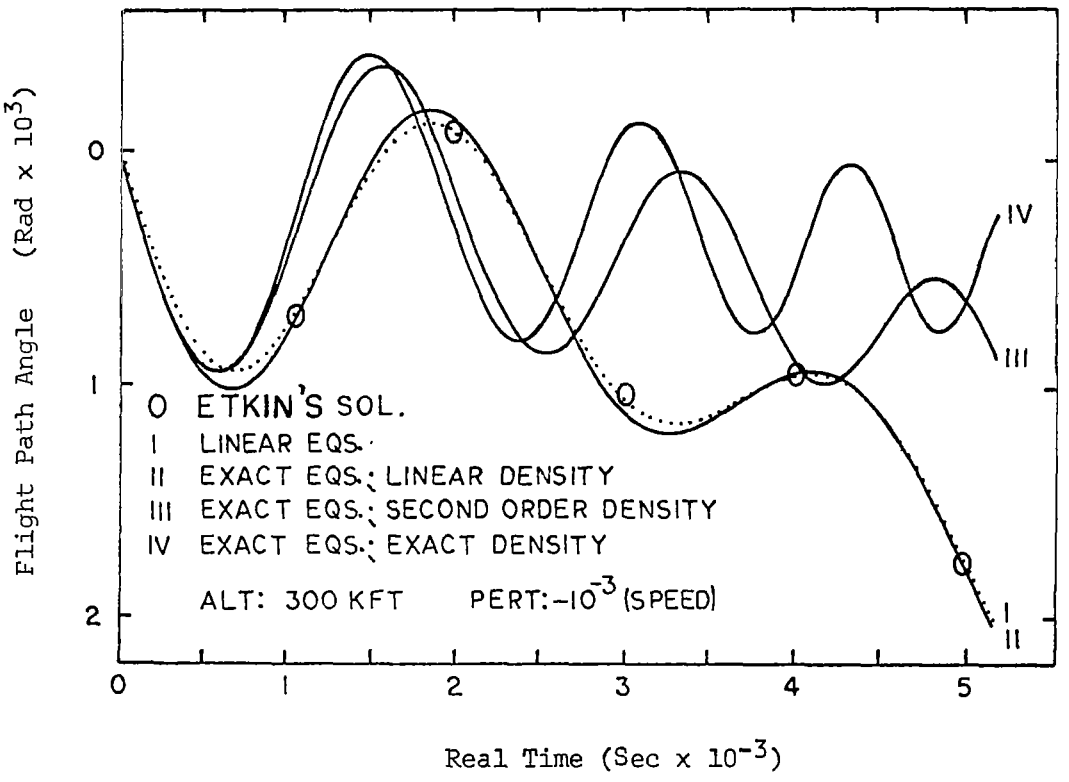

Fig. C-2 Variation of Flight Path Angle

is about 2 linear periods. Referring to Fig. C-2 the flight path angle time history shows that the exact integration curve displays less spiral mode and less damping than the linear solution and further shows that the exact phugoid oscillations have smaller period. In fact the first cycle takes 1.95×10^3 secs versus the linear phugoid period of 2.51×10^3 secs. The second and third cycles take even less time and show that the exact motion will complete 3 cycles for the two linear periods.

A complete numerical analysis shows that below 100,000 ft or above 400,000 ft linear solutions are accurate. In between there is a definite requirement for the inclusion of higher order atmospheric mass density gradients.